NASA Contractor Report 164058

APPLICATION OF THE LINE-SPRING MODEL TO A CYLINDRICAL SHELL CONTAINING A CIRCUMFERENTIAL OR AXIAL PART-THROUGH CRACK

F. Delale and F. Erdogan

LEHIGH UNIVERSITY
Bethlehem, Pennsylvania 18015

Grant NGR 39-007-011
April 1981

National Aeronautics and Space Administration

Langley Research Center
Hampton, Virginia 23665

"APPLICATION OF THE LINE-SPRING MODEL TO A CYLINDRICAL SHELL CONTAINING A CIRCUMFERENTIAL OR AXIAL PART-THROUGH CRACK"(*)

by

F. Delale and F. Erdogan

Lehigh University, Bethlehem, PA. 18015

Abstract

In this paper the line-spring model developed by Rice and Levy is used to obtain an approximate solution for a cylindrical shell containing a part-through surface crack. It is assumed that the shell contains a circumferential or axial semi-elliptic internal or external surface crack and is subjected to a uniform membrane loading or a uniform bending moment away from the crack region. To formulate the shell problem, a Reissner type theory is used in order to account for the effects of the transverse shear deformations. The stress intensity factor at the deepest penetration point of the crack is tabulated for bending and membrane loading by varying three dimensionless length parameters of the problem formed from the shell radius, the shell thickness, the crack length, and the crack depth. The upper bounds of the stress intensity factors are provided by the results of the elasticity solution obtained from the axisymmetric crack problem for the circumferential crack, and that found from the plane strain problem for a circular ring having a radial crack for the axial crack. Qualitatively the line-spring model gives the expected results in comparison with the elasticity solutions. The results also compare well with the existing finite element solution of the pressurized cylinder containing an internal semi-elliptic surface crack.

1. Introduction

In recent years there has been some renewed interest in the line-spring model which was developed in [1] for obtaining an approximate solution of a plate containing a part-through surface crack. There are

(*) This work was supported by the Department of Transportation under the contract DOT-RC-82007, by NSF under the Grant CME-78-08737, and by NASA-Langley under the Grant NGR 39-007-011.

a number of reasons for this. First, the accuracy of the results obtained from the model turned out to be better than that shown by the early comparisons with the solutions found from the finite element and the alternating methods [2-6] (see, for example, [7]). Secondly, the technique appears to have the potential for important applications to a great variety of shell structures of rather complex geometries with a relatively small computational effort. Finally, it can be quite useful to study certain aspects of the part-through crack problem in the presence of large scale plastic deformations (see, for example, the interesting recent work by Parks [7,9], and [8] and [10]).

In this paper the elastic problem for a relatively thin-walled cylinder containing a semi-elliptic part-through crack is considered. It is assumed that the crack lies in a plane perpendicular to or containing the axis of the cylinder and may be an external or an internal surface crack. In formulating the problem, the cylinder is approximated by a shallow shell and the effect of transverse shear deformations are taken into account [11,12]. The edge-cracked strip results used in the line-spring model are obtained from an integral equation solution given in [13].

The stress intensity factor for a part-through axial crack located inside the cylinder is given in [14-16] where in [14] and [15] the finite element and in [16] the boundary integral equation method is used to solve the problem. The results found in this paper are compared with those given in [14] as well as the related plane strain and axisymmetric elasticity solutions. The stress intensity factors obtained from the elasticity solutions for a ring with a radial crack under plane strain conditions and for a cylinder containing an axisymmetric circumferential surface crack provide upper bounds for the results corresponding to an axial and a circumferential surface crack of finite length.

2. General Formulation

The part-through crack geometry for the cylindrical shell under consideration is shown in Figure 1. It is assumed that the external loads are symmetric with respect to the plane of the crack. Thus, the only nonzero net ligament stress and moment resultants which have a constraining effect on the crack surface displacements would be the membrane resultant N_{11} and the moment resultant M_{11}. The basic idea underlying the line-spring model consists of (a) representing the net ligament stresses by a membrane load N and a bending moment M, and the crack surface displacements by a crack opening δ and a relative rotation θ, all referred to the midplane of the shell and continuously distributed along the length of the crack, (b) approximating the relationship between (N,M) and (δ,θ) by the corresponding plane strain results obtained from the solution of an edge-cracked strip or a ring, and (c) reducing the problem to a pair of integral equations for the unknown functions N and M or δ and θ by using the boundary and the continuity conditions for the shell in the plane of the crack.

In the formulation of the crack problem for the shell, the derivatives of the crack surface displacement and rotation are used as the unknown functions which are defined by

$$\frac{\partial}{\partial y} u(+0,y) = G_1(y) \ , \ \frac{\partial}{\partial y} \beta_x(+0,y) = G_2(y) \quad . \tag{1a,b}$$

The notation and the dimensionless quantities used in the formulation are given in Figure 1 and in Appendix A. It is shown in [17] that the general problem for a symmetrically loaded shell containing a through crack may be reduced to the following system of integral equations:

$$\int_{-1}^{1} \frac{G_1(t)}{t-y}\,dt + \int_{-1}^{1} \sum_{1}^{2} k_{1j}(y,t)G_j(t)dt = 2\pi F_1(y), \ -1 < y < 1, \tag{2a}$$

$$\frac{1-\nu^2}{\lambda^4} \int_{-1}^{1} \frac{G_2(t)}{t-y}\,dt + \int_{-1}^{1} \sum_{1}^{2} k_{2j}(y,t)G_j(t)dt = 2\pi \frac{h}{a} F_2(y), \ -1<y<1, \tag{2b}$$

$$k_{11}(y,t) = \int_0^\infty [2 \sum_1^4 \alpha^2 Q_j(\alpha) - 1] \sin\alpha(t-y)d\alpha \ ,$$

$$k_{12}(y,t) = \int_0^\infty 2\alpha^2 \sum_1^4 N_j(\alpha)\sin\alpha(t-y)d\alpha \ ,$$

$$k_{21}(y,t) = -\frac{2}{\lambda^2}\int_0^\infty \sum_1^4 \frac{p_j^2(m_j^2-\nu\alpha^2)Q_j(\alpha)}{(\kappa p_j-1)(\lambda_2^2 m_j^2-\lambda_1^2\alpha^2)} \sin\alpha(t-y)d\alpha \ ,$$

$$k_{22}(y,t) = -\frac{2}{\lambda^4}\int_0^\infty [\lambda^2 \sum_1^4 \frac{p_j^2(m_j^2-\nu\alpha^2)N_j(\alpha)}{(\kappa p_j-1)(\lambda_2^2 m_j^2-\lambda_1^2\alpha^2)}$$

$$- \kappa(1-\nu)^2\alpha r_1 + (1-\nu^2)/2]\sin\alpha(t-y)d\alpha \qquad (3a\text{-}d)$$

subject to

$$\int_{-1}^{1} G_1(y)dy = 0 \ , \quad \int_{-1}^{1} G_2(y)dy = 0 \ . \qquad (4a,b)$$

The problem is formulated as a stress disturbance problem in which a homogeneous stress solution for the uncracked shell is separated through a superposition and it is assumed that the stress and moment resultants applied to the crack surfaces are the only external loads. Thus, F_1 and F_2 appearing in (2) are

$$F_1(y) = N_{xx}(+0,y) \ , \ F_2(y) = M_{xx}(+0,y), \ -1<y<1 \ . \qquad (5a,b)$$

The parameters r_1, m_j, and p_j, (j=1,...,4) are functions of the transform variable α and are given by

$$r_1 = -\left[\alpha^2 + \frac{2}{\kappa(1-\nu)}\right]^{1/2} \ , \qquad (6)$$

$$m_j^2 = p_j + \alpha^2 \ , \ \mathrm{Re}(m_j) < 0, \ (j=1,...,4) \ , \qquad (7)$$

and $p_1,\ldots,p_4$ are the roots of

$$p^4 - \kappa\lambda_2^4 p^3 + (2\kappa\lambda_1^2\lambda_2^2\alpha^2 - 2\kappa\lambda_2^4\alpha^2 + \lambda_2^4)p^2 + (2\kappa\lambda_1^2\lambda_2^2\alpha^2 - \kappa\lambda_2^4\alpha^2$$

$$- \kappa\lambda_1^4\alpha^2 + 2\lambda_2^4 - 2\lambda_1^2\lambda_2^2)\alpha^2 p + (\lambda_2^2-\lambda_1^2)^2\,\alpha^4 = 0 \qquad (8)$$

From (6-8) it may be shown that for large values of $|\alpha|$ we have

$$r_1(\alpha) = -|\alpha|\,[1 + \frac{1}{\kappa(1-\nu)\alpha^2} + O(\frac{1}{\alpha^4})]\,, \qquad (9)$$

$$m_j(\alpha) = -|\alpha|\,[1 + \frac{p_j}{2\alpha^2} - \frac{p_j^2}{8\alpha^4} + O(\frac{1}{\alpha^6})]\,, \qquad (10)$$

where the roots p_j of the characteristic equation (8) are bounded for all values of α.

The functions Q_j and N_j, $(j=1,\ldots,4)$ which appear in the kernels (3) are found from

$$R_j(\alpha) = i[Q_j(\alpha)f_1(\alpha) + N_j(\alpha)f_2(\alpha)]\,,\ (j = 1,\ldots,4)\,, \qquad (11)$$

where

$$f_k(\alpha) = \int_{-1}^{1} G_k(t)e^{i\alpha t}\,dt,\ (k=1,2) \qquad (12)$$

and $R_1,\ldots,R_4$ are obtained from

$$\sum_1^4 m_j R_j(\alpha) = 0\,,$$

$$\sum_1^4 \frac{R_j(\alpha)(\lambda_2^2 p_j^2 m_j - \lambda_2^2 m_j^5 + \lambda_1^2\alpha^2 m_j^3)}{\lambda_2^2 m_j^2 - \lambda_1^2\alpha^2} = -i\alpha f_1(\alpha)\,,$$

$$\sum_1^4 \frac{R_j(\alpha)p_j^2 m_j}{(\kappa p_j - 1)(\lambda_2^2 m_j^2 - \lambda_1^2\alpha^2)} = \frac{i(1-\nu)\kappa}{2\alpha\lambda^2}\,(r_1^2+\alpha^2)f_2(\alpha)\,,$$

$$\sum_1^4 \frac{R_j(\alpha)p_j^3 m_j}{(\kappa p_j - 1)(\lambda_2^2 m_j^2 - \lambda_1^2\alpha^2)} = \frac{i(1-\nu)}{\lambda^2}\,\alpha f_2(\alpha)\,, \qquad (13a\text{-}d)$$

The formulation given above refer to a shallow shell containing a crack along the principal plane of curvature coinciding with X_2X_3 plane (Figure 1). The principal radii of curvature R_1 and R_2 are defined by

$$\frac{1}{R_1} = -\frac{\partial^2 Z}{\partial X_1^2} , \frac{1}{R_2} = -\frac{\partial^2 Z}{\partial X_2^2} , \qquad (14a,b)$$

where $Z(X_1,X_2)$ is the distance of the point on the middle surface to the tangent plane X_1X_2. Thus, for the circumferential crack shown in Figure 1a, $R_2=R$ and $R_1=\infty$ (giving $\lambda_1=0$), and for the axial crack shown in Figure 1b $R_1=R$ and $R_2=\infty$ (giving $\lambda_2=0$).

Let now

$$N_{11} = N_\infty , M_{11} = M_\infty \qquad (15a,b)$$

be the uniform membrane load and the bending moment applied to the shell away from the crack region and $N(X_2)$ and $M(X_2)$ the stress and moment resultants which are equivalent to the net ligament stresses in $-a<X_2<a$ or $-1<y<1$. The "input" functions which appear in the integral equations (2) may then be expressed as

$$F_1(y) = \frac{1}{E}(-\sigma_\infty+\sigma) , F_2(y) = \frac{1}{6E}(-m_\infty+m) , \qquad (16a,b)$$

for the crack located on the outside and

$$F_1(y) = \frac{1}{E}(-\sigma_\infty+\sigma) , F_2(y) = \frac{1}{6E}(m_\infty-m) , \qquad (17a,b)$$

for the crack located inside the cylinder(*) where

$$\sigma_\infty = \frac{N_\infty}{h} , m_\infty = \frac{6M_\infty}{h^2} , \qquad (18a,b)$$

(*) In both cases the applied moment M is such that the crack tends to open under bending of the shell, and the net ligament moment is assumed to constrain the crack surface rotation, hence the change in sign of F_2 in (16) and (17).

and

$$\sigma(y) = \frac{N(X_2)}{h} = \frac{N(ay)}{h} \ , \ m(y) = \frac{6M(X_2)}{h^2} = \frac{6M(ay)}{h^2} \ . \qquad (19a,b)$$

The stresses σ and m are linearly related to the crack surface displacement a $u(+0,y) = \delta/2$ and rotation $\beta_x(+0,y) = \theta/2$. This relationship may be obtained from the related plane strain problem by expressing the rate of change of the potential energy in terms of the crack closure energy and the change in gross compliance as follows:

$$\frac{1-\nu^2}{E} K^2 = \frac{1}{2} \left[\sigma h \frac{\partial \delta}{\partial L} + \frac{mh^2}{6} \frac{\partial \theta}{\partial L}\right] \qquad (20)$$

where K is the total mode I stress intensity factor at the crack tip and L is the length of the edge crack. If we now let

$$K = \sqrt{h} \ (\sigma \ g_t + m \ g_b) \ , \qquad (21)$$

from (20) we obtain

$$\sigma(y) = E[\gamma_{tt}(y)u(+0,y) \pm \gamma_{tb}(y)\beta_x(+0,y)] \ ,$$

$$m(y) = 6E[\gamma_{bt}(y)u(+0,y) \pm \gamma_{bb}(y)\beta_x(+0,y)] \ , \qquad (22a,b)$$

where + and - signs are to be used for the outer and the inner cracks, respectively and

$$\gamma_{tt} = \frac{a}{h(1-\nu^2)} \frac{\alpha_{bb}}{\Delta} \ , \ \gamma_{bb} = \frac{1}{36(1-\nu^2)} \frac{\alpha_{tt}}{\Delta} \ ,$$

$$\gamma_{tb} = -\frac{1}{6(1-\nu^2)} \frac{\alpha_{tb}}{\Delta} \ , \ \gamma_{bt} = -\frac{a}{6h(1-\nu^2)} \frac{\alpha_{bt}}{\Delta} \ ,$$

$$\Delta = \alpha_{tt} \alpha_{bb} - \alpha_{tb}^2 \ , \qquad (23a\text{-}e)$$

$$\alpha_{ij} = \frac{1}{h} \int_0^L g_i g_j \, dL \ , \ (i,j = t,b) \ . \qquad (24)$$

The crack depth L is assumed to be a known function of y (Figure 1).

Referring to the definitions (1), u and β_x may be expressed as

$$u(+0,y) = \int_{-1}^{y} G_1(t)dt \ , \ \beta_x(+0,y) = \int_{-1}^{y} G_2(t)dt \ . \qquad (25a,b)$$

Substituting from (25) and (22) into (2) the final form of the integral equations is found to be

$$-\gamma_{tt}(y)\int_{-1}^{y} G_1(t)dt \mp \gamma_{tb}(y)\int_{-1}^{y} G_2(t)dt + \frac{1}{2\pi}\int_{-1}^{1} \frac{G_1(t)}{t-y}\,dt$$

$$+ \frac{1}{2\pi}\int_{-1}^{1}[k_{11}(y,t)G_1(t) + k_{12}(y,t)G_2(t)]dt = -\frac{\sigma_\infty}{E} \ , \ -1<y<1 \ ,$$

$$\mp\gamma_{bt}(y)\int_{-1}^{y} G_1(t)dt - \gamma_{bb}(y)\int_{-1}^{y} G_2(t)dt + \frac{a(1-\nu^2)}{2\pi h\lambda^4}\int_{-1}^{1} \frac{G_2(t)}{t-y}\,dt$$

$$+ \frac{a}{2\pi h}\int_{-1}^{1}[k_{21}(y,t)G_1(t) + k_{22}(y,t)G_2(t)]dt = \mp\frac{m_\infty}{6E} \ , \ -1<y<1$$

(26a,b)

where the upper (i.e., -) and the lower (i.e., +) signs are to be used for the outer and the inner crack, respectively.

3. Compliance Coefficients

The functions g_t and g_b which appear in (21) and which give the membrane and bending components of the stress intensity factor are obtained from the corresponding plane strain crack geometry.

For the circumferential crack, the appropriate geometry is that of an infinite strip with an edge crack. On the other hand, for the axial crack the proper plane strain problem would be that of a ring having a radial edge crack. In a recent study the ring problem was formulated in terms of a singular integral equation [18]. The results

given in [18] show that for cylinders with values of h/R which may be considered a "shallow shell", the ring results are reasonably close to the strip results. Also for small values of h/R the convergence of the numerical solution of the ring problem is not very good. Hence, the complete parametrization of the problem for the purpose of obtaining g_t and g_b (which would be functions of h/R as well as L/h) becomes rather complicated. In this paper, therefore, the edge-cracked strip results will be used for both the axial and the circumferential crack problem.

For the strip the functions g_t and g_b are obtained from the results given in [13] which are valid for $0<L/h<0.8$ and may be expressed as

$$g_t(\xi) = \sqrt{\pi\xi}\,(1.1216 + 6.5200\xi^2 - 12.3877\xi^4 + 89.0554\xi^6 - 188.6080\xi^8 + 207.3870\xi^{10} - 32.0524\xi^{12}]\,,$$

$$g_b(\xi) = \sqrt{\pi\xi}\,(1.1202 - 1.8872\xi + 18.0143\xi^2 - 87.3851\xi^3 + 241.9124\xi^4 - 319.9402\xi^5 + 168.0105\xi^6) \qquad (27a,b)$$

where $\xi = L(X_2)/h = L(ay)/h$. From (27) and (24) the functions α_{ij}, (i,j=t,b) may be determined as follows:

$$\alpha_{tt} = \xi^2 \sum_{n=0}^{12} C_{tt}^{(n)}\,\xi^{2n}\,,\quad \alpha_{bb} = \xi^2 \sum_{n=0}^{12} C_{bb}^{(n)}\,\xi^{n}\,,$$

$$\alpha_{tb} = \alpha_{bt} = \xi^2 \sum_{n=0}^{18} C_{tb}^{(n)}\,\xi^{n}\,. \qquad (28a\text{-}c)$$

The coefficients $C_{ij}^{(n)}$ are given in Table 1.

4. Solution for the Cylindrical Shell

The solution of the problem is obtained for a uniform membrane loading N_∞ and for a bending moment M_∞ applied to the shell away from the crack region and for the Poisson's ratio $\nu = 0.3$. Even though $L(X_2) = L(ay)$ describing the crack shape can be any single-valued function, the problem is solved only for a semi-elliptic surface crack given by

$$L = L_0\sqrt{1-(X_2/a)^2} = L_0\sqrt{1-y^2} \quad . \tag{29}$$

The solution of the integral equations (26) is of the form

$$G_i(t) = \frac{\phi_i(t)}{(1-t^2)^{\frac{1}{2}}} \ , \ (i=1,2) \ (-1<t<1) \tag{30}$$

where ϕ_1 and ϕ_2 are bounded functions. The functions ϕ_i may be determined from (26) to any desired degree of accuracy by using the Gauss-Chebyshev integration procedure [19]. After obtaining ϕ_1 and ϕ_2 the unknowns σ and m representing the net ligament stresses may be determined from (22) by using (23-25), (27) and (28). The stress intensity factor K(y) may then be obtained from (21) and (27). For a Poisson's ratio $\nu = 0.3$ and for various crack geometries and loading conditions the calculated results are shown in Figures 2-7 and Tables 2-11. Tables 2-9 give the normalized stress intensity factor at the deepest penetration point y=0, $L=L_0$ of a semi-elliptic surface crack in a cylindrical shell under uniform membrane loading or bending. The normalizing stress intensity factor k_0 is the corresponding value for the plane strain problem under tension or bending and is given by

$$k_0 = \frac{K_0}{\sqrt{\pi}} = \frac{N_\infty}{\sqrt{\pi}\ h}\sqrt{h}\ g_t(\xi_0) \ , \ \xi_0 = \frac{L_0}{h} \ , \tag{31}$$

for membrane loading, and

$$k_o = \frac{K_o}{\sqrt{\pi}} = \frac{6M_\infty}{h^2\sqrt{\pi}} \sqrt{h}\, g_b(\xi_o),\ \xi_o = \frac{L_o}{h} \tag{32}$$

for bending.

Figures 2 and 3 show the comparison of the shell results with the stress intensity factors obtained from the corresponding axisymmetric and plane strain problems. As $(R_i/R_o) \to 1$ the shell results approach the flat plate solution k_p [21] having a part-through semi-elliptic crack of the same geometry and relative dimensions. It may be noted that, as expected, the shell stress intensity factors are generally smaller than the corresponding two-dimensional values. Even though the shell results are given for $0.74<(R_i/R_o)<1$, because of the nature of the theory used in the shell analysis, namely the shallow shell theory, for $(R_i/R_o) < 0.9$ the results may not be very accurate. From Figure 3 one may also observe that the difference between shell and the plane strain results decrease with decreasing crack depth (L_o/h)*.

Some sample results for the distribution of the stress intensity factor along the crack front are given in Tables 10 and 11 and in Figures 4-6. The normalization factors k_o used in these tables and figures are also those given by (31) and (32). The variable ϕ used in the presentation of these results is the usual parametric angle of the ellipse shown in the insert of Figure 4. For small values of ϕ the stress intensity factors given by the line-spring model are neither reliable nor meaningful and therefore are not presented.

The only shell results which exist in literature and which are obtained by using a method other than that of the line-spring are the stress intensity factors in a pressurized cylinder containing an internal semi-elliptic axial crack [14-16]. Figure 7 shows the comparison of the stress intensity factors obtained from the line-spring model and those given in [14] which are found by using the finite element method. The parameter ϕ is again defined by the insert in

(*) The plane strain cylinder results given in Figure 3 are obtained from [18] and the axisymmetric crack results shown in Figure 2 are from [20].

Figure 4. The stress intensity factor ratio F shown in Figure 7 is defined by

$$F = \frac{K}{\frac{pR_i}{h}\sqrt{\pi L_o/Q}} \quad , \tag{33}$$

where $K = k\sqrt{\pi}$ is the stress intensity factor along the crack front, p is the internal pressure and $Q = [E(k)]^2$, E being the complete elliptic integral of the second kind. The results given in Figure 7 include the effect of the pressure p acting on the crack surface. Considering the gross approximations involved in the formulation of the problem by using the line-spring model, and the fact that the finite element results themselves may contain a few percent error, the agreement between the two results seems to be quite good. The plane strain results given in Figure 3 suggest that the accuracy of the results given by the line-spring model could perhaps be improved further if the ring rather than the flat plate solution is used to derive the functions g_t and g_b to express the stress intensity factor (see equations (21) and (27)).

REFERENCES

1. Rice, J.R. and Levy, N., "The Part-Through Surface Crack in an Elastic Plate," Journal of Applied Mechanics, V. 39, 1972, pp. 185-194.

2. Raju, I.S. and Newman, J.C., Jr., "Stress-Intensity Factors for a Wide Range of Semi-Elliptical Surface Cracks in Finite-Thickness Plates", Journal of Engr. Fracture Mechanics, Vol. 11, pp. 817-829, 1979.

3. Newman, J.C., Jr., A Review and Assessment of the Stress-Intensity Factors for Surface Cracks, NASA, Technical Memorandum 78805, Nov. 1978.

4. Atluri, S.N., Kathiresan, K., Kobayashi, A.S., and Nakagaki, M., "Inner Surface Cracks in an Internally Pressurized Cylinder Analyzed by a Three-Dimensional Displacement-Hybrid Finite Element Method", Proc. of the Third Int. Conf. on Pressure Vessel Technology, Part III, pp. 527-533, ASME, New York, 1977.

5. Smith, F.W. and Sorensen, D.R., "The Semi-Elliptical Surface Crack - A Solution by the Alternating Method", Int. J. of Fracture, Vol. 12, pp. 47-57, 1976.

6. Shah, R.C. and Kobayashi, A.S., On the Surface Flaw Problem, The Surface Crack: Physical Problems and Computational Solutions, ed. J.L. Swedlow, 1972, pp. 79-124.

7. Parks, D.M., "The Inelastic Line-Spring: Estimates of Elastic-Plastic Fracture Mechanics Parameters for Surface-Cracked Plates and Shells", Paper 80-C2/PVP-109, ASME, 1980.

8. Rice, J.R., "The Line-Spring Model for Surface Flaws", The Surface Crack: Physical Problems and Computational Solutions", ed. J.L. Swedlow, pp. 171-185, ASME, New York, 1972.

9. Parks, D.M., "Inelastic Analysis of Surface Flaws Using the Line-Spring Model", Proceedings of the 5th International Conference on Fracture, Cannes, France, 1981.

10. Erdogan, F. and Ratwani, M., "Plasticity and Crack Opening Displacement in Shells", Int. J. of Fracture Mechanics, Vol. 8, pp. 413-426, 1972.

11. Reissner, E. and Wan, F.Y.M., "On the Equations of Linear Shallow Shell Theory", Studies in Applied Mathematics, Vol. 48, pp. 132-145, 1969.

12. Naghdi, P.M., "Note on the Equations of Elastic Shallow Shells", Quart. Appl. Math., Vol. 14, pp. 331-333 (1956).

13. Kaya, A.C. and Erdogan, F., "Stress Intensity Factors and COD in an Orthotropic Strip", Int. J. Fracture, Vol. 16, pp. 171-190, 1980.

14. Newman, J.C. and Raju, I.S., "Stress Intensity Factors for Internal Surface Cracks in Cylindrical Pressure Vessels", NASA Technical Memorandum 80073, July 1979.

15. McGowan, J.J. and Raymund, M., "Stress Intensity Factor Solutions for Internal Longitudinal Semi-Elliptical Surface Flaws in a Cylinder under Arbitrary Loadings", Fracture Mechanics, ASTM, STP 677, 1979.

16. Heliot, J. and Labbens, R.C. and Pellisier-Tanon, A., "Semi-Elliptic Cracks in a Cylinder Subjected to Stress Gradients", Fracture Mechanics, ASTM, STP 677, pp. 341-364, 1979.

17. Delale, F. and Erdogan, F., "Effect of Transverse Shear and Material Orthotropy in a Cracked Spherical Cap", Int. J. Solids Structures, Vol. 15, pp. 907-926, 1979.

18. Delale, F. and Erdogan, F., "Stress Intensity Factors in a Hollow Cylinder Containing a Radial Crack", NASA Project Report, NGR 39-007-011, November 1980.

19. Erdogan, F., "Mixed Boundary-Value Problems in Mechanics", Mechanics Today, Nemat-Nasser, S., ed., Vol. 4, Pergamon Press, Oxford, pp. 1-86, 1978.

20. Nied, H.F., "A Hollow Cylinder with an Axisymmetric Internal or Surface Crack under Nonaxisymmetric Arbitrary Loading", Ph.D. Dissertation, Lehigh University, June 1981.

21. Delale, F. and Erdogan, F., "Line-Spring Model for Surface Cracks in a Reissner Plate", NASA, Technical Report, Lehigh University, November 1980.

APPENDIX A

The notation and dimensionless quantities (Fig. 1)

$$x = \frac{X_1}{a} \quad , \quad y = \frac{X_2}{a} \quad , \quad z = \frac{X_3}{a} \quad , \tag{A.1}$$

$$u = \frac{U_1}{a} \quad , \quad v = \frac{U_2}{a} \quad , \quad w = \frac{W}{a} \quad , \tag{A.2}$$

$$\beta_x = \beta_1 \quad , \quad \beta_y = \beta_2 \quad , \tag{A.3}$$

$$N_{xx} = \frac{N_{11}}{hE} \quad , \quad N_{yy} = \frac{N_{22}}{hE} \quad , \quad N_{xy} = \frac{N_{12}}{hE} \tag{A.4}$$

$$M_{xx} = \frac{M_{11}}{h^2E} \quad , \quad M_{yy} = \frac{M_{22}}{h^2E} \quad , \quad M_{xy} = \frac{M_{12}}{h^2E} \tag{A.5}$$

$$V_x = \frac{V_1}{hB} \quad , \quad V_y = \frac{V_2}{hB} \quad , \tag{A.6}$$

$$\lambda_1^4 = 12(1-\nu^2)\frac{a^4}{h^2R_1^2} \quad , \quad \lambda_2^4 = 12(1-\nu^2)\frac{a^4}{h^2R_2^2} \quad ,$$

$$B = \frac{5}{6}\frac{E}{2(1+\nu)} \quad , \quad \lambda^4 = 12(1-\nu^2)\frac{a^2}{h^2} \quad , \quad \kappa = \frac{E}{B\lambda^4} \tag{A.7}$$

U_1, U_2, W: components of the displacement vector,

β_1, β_2: rotations of the normal,

N_{ij}, (i,j=1,2): Membrane stress resultants

M_{ij}, (i,j=1,2): Moment resultants

V_i, (i=1,2): Transverse shear resultants

R_1, R_2: Principal radii of curvature

Table 1. Coefficients $C_{ij}^{(n)}$ which appear in eqs. (28)

n	$C_{tt}^{(n)}$	$C_{tb}^{(n)}$	$C_{bb}^{(n)}$
0	1.9761	1.9735	1.9710
1	11.4870	-2.2166	-4.4277
2	7.7086	21.6051	34.4952
3	15.0143	-69.3133	-165.7321
4	280.1207	196.3000	626.3926
5	-1099.7200	-406.2608	-2144.4651
6	3418.9795	644.9350	7043.4169
7	-7686.9237	-408.9569	-19003.2199
8	12794.1279	-159.6927	37853.3028
9	-13185.0403	-988.9879	-52595.4681
10	7868.2682	4266.5487	48079.2948
11	-1740.2463	-2997.1408	-25980.1559
12	124.1360	-6050.7849	6334.2425
13		8855.3615	
14		3515.4345	
15		-11744.1116	
16		4727.9784	
17		1695.6087	
18		-845.8958	

Table 2. Normalized stress intensity factor k/k_0 at the deepest penetration point $L=L_0$, $y=0$ of an outer semielliptic circumferential crack in a cylinder under uniform membrane loading N_∞; $\lambda_2 = [12(1-\nu^2)]^{1/4}\, a/\sqrt{Rh}$, $\nu=0.3$.

	$L_0 = 0.2h$				$L_0 = 0.4h$			
λ_2	a=h	a=2h	a=4h	a=8h	a=h	a=2h	a=4h	a=8h
0	0.817	0.883	0.930	0.961	0.507	0.627	0.741	0.837
0.5	0.817	0.883	0.930	0.961	0.509	0.628	0.742	0.837
0.75	0.816	0.882	0.930	0.961	0.509	0.628	0.742	0.837
1.0		0.880	0.929	0.960		0.626	0.741	0.836
1.5		0.876	0.926	0.959		0.620	0.736	0.833
2.0			0.922	0.956			0.727	0.827
4.0			0.893	0.939			0.670	0.784
6.0				0.916				0.728
8.0				0.893				0.676
	$L_0 = 0.6h$				$L_0 = 0.8h$			
0	0.245	0.336	0.451	0.582	0.073	0.104	0.149	0.216
0.5	0.248	0.339	0.454	0.583	0.074	0.106	0.151	0.219
0.75	0.250	0.341	0.455	0.585	0.076	0.107	0.152	0.220
1.0		0.341	0.455	0.585		0.109	0.154	0.221
1.5		0.341	0.453	0.583		0.112	0.157	0.223
2.0			0.448	0.577			0.158	0.224
4.0			0.408	0.532			0.158	0.214
6.0				0.476				0.197
8.0				0.428				0.182

Table 3. Normalized stress intensity factor k/k_0 at the deepest penetration point $L=L_0$, $y=0$ of an outer semi-elliptic circumferential crack in a cylindrical shell under uniform bending moment M_∞.

	$L_0 = 0.2h$				$L_0 = 0.4h$			
λ_2	a=h	a=2h	a=4h	a=8h	a=h	a=2h	a=4h	a=8h
0	0.804	0.875	0.926	0.959	0.441	0.579	0.710	0.819
0.5	0.804	0.875	0.926	0.959	0.443	0.581	0.712	0.819
0.75	0.803	0.874	0.925	0.958	0.443	0.580	0.711	0.819
1.0		0.872	0.924	0.958		0.578	0.709	0.818
1.5		0.867	0.921	0.956		0.570	0.703	0.814
2.0			0.916	0.953			0.692	0.806
4.0			0.884	0.934			0.621	0.753
6.0				0.909				0.686
8.0				0.883				0.624
	$L_0 = 0.6h$				$L_0 = 0.8h$			
0	0.132	0.238	0.373	0.526	-0.012	0.017	0.065	0.140
0.5	0.135	0.241	0.376	0.529	-0.010	0.019	0.068	0.143
0.75	0.137	0.243	0.377	0.529	-0.008	0.021	0.069	0.145
1.0		0.243	0.377	0.529		0.023	0.071	0.146
1.5		0.242	0.374	0.526		0.027	0.074	0.148
2.0			0.367	0.519			0.075	0.148
4.0			0.313	0.459			0.072	0.132
6.0				0.386				0.108
8.0				0.326				0.088

Table 4. Normalized stress intensity factor k/k_0 at the deepest penetration point $y=0$, $L=L_0$ of an inner semi-elliptic circumferential surface crack in a cylindrical shell under uniform membrane loading N_∞.

	$L_0 = 0.2h$				$L_0 = 0.4h$			
λ_2	a=h	a=2h	a=4h	a=8h	a=h	a=2h	a=4h	a=8h
0	0.817	0.883	0.930	0.961	0.507	0.627	0.741	0.837
0.5	0.810	0.879	0.928	0.960	0.497	0.618	0.735	0.833
0.75	0.804	0.875	0.926	0.959	0.487	0.610	0.729	0.829
1.0		0.870	0.923	0.957		0.600	0.722	0.824
1.5		0.858	0.916	0.953		0.579	0.704	0.812
2.0			0.907	0.948			0.685	0.798
4.0			0.870	0.926			0.613	0.739
6.0				0.902				0.687
8.0				0.881				0.646
	$L_0 = 0.6h$				$L_0 = 0.8h$			
0	0.245	0.336	0.451	0.582	0.073	0.104	0.149	0.216
0.5	0.240	0.330	0.444	0.576	0.073	0.103	0.147	0.213
0.75	0.236	0.324	0.438	0.570	0.073	0.102	0.145	0.210
1.0		0.318	0.431	0.563		0.101	0.143	0.207
1.5		0.305	0.414	0.546		0.101	0.140	0.200
2.0			0.398	0.529			0.137	0.194
4.0			0.350	0.467			0.133	0.177
6.0				0.422				0.168
8.0				0.392				0.163

Table 5. Normalized stress intensity factor k/k_0 at the deepest penetration point y=0, $L=L_0$ of an inner semi-elliptic circumferential surface crack in a cylindrical shell under uniform bending moment M_∞.

	$L_0 = 0.2h$				$L_0 = 0.4h$			
λ_2	a=h	a=2h	a=4h	a=8h	a=h	a=2h	a=4h	a=8h
0	0.804	0.875	0.926	0.959	0.441	0.579	0.710	0.819
0.5	0.797	0.870	0.923	0.957	0.429	0.569	0.703	0.814
0.75	0.789	0.866	0.921	0.956	0.418	0.559	0.696	0.809
1.0		0.860	0.917	0.954		0.547	0.687	0.803
1.5		0.847	0.909	0.950		0.522	0.666	0.789
2.0			0.900	0.945			0.643	0.772
4.0			0.859	0.920			0.557	0.702
6.0				0.894				0.640
8.0				0.871				0.592
	$L_0 = 0.6h$				$L_0 = 0.8h$			
0	0.132	0.238	0.373	0.526	-0.012	0.017	0.065	0.140
0.5	0.125	0.230	0.364	0.518	-0.013	0.015	0.062	0.136
0.75	0.119	0.222	0.356	0.511	-0.013	0.014	0.060	0.133
1.0		0.214	0.347	0.502		0.013	0.057	0.129
1.5		0.197	0.326	0.481		0.012	0.053	0.120
2.0			0.306	0.460			0.049	0.112
4.0			0.244	0.382			0.042	0.089
6.0				0.327				0.078
8.0				0.289				0.070

Table 6. Normalized stress intensity factor k/k_0 at the deepest penetration point y=0, $L=L_0$ of an outer semi-elliptic axial surface crack in a cylindrical shell under uniform membrane loading N_∞

	$L_0 = 0.2h$				$L_0 = 0.4h$			
λ_1	a=h	a=2h	a=4h	a=8h	a=h	a=2h	a=4h	a=8h
0	0.817	0.883	0.930	0.961	0.507	0.627	0.741	0.837
0.5	0.822	0.886	0.932	0.962	0.518	0.635	0.748	0.841
0.75	0.826	0.888	0.933	0.963	0.527	0.642	0.752	0.844
1.0		0.890	0.934	0.963		0.649	0.757	0.847
1.5		0.894	0.936	0.964		0.663	0.766	0.853
2.0			0.938	0.965			0.773	0.857
4.0			0.935	0.964			0.775	0.860
6.0				0.959				0.848
8.0				0.954				0.834
	$L_0 = 0.6h$				$L_0 = 0.8h$			
0	0.245	0.336	0.451	0.582	0.073	0.104	0.149	0.216
0.5	0.255	0.346	0.461	0.590	0.076	0.108	0.154	0.223
0.75	0.264	0.355	0.468	0.597	0.080	0.112	0.159	0.229
1.0		0.364	0.477	0.604		0.118	0.165	0.235
1.5		0.384	0.494	0.619		0.130	0.178	0.250
2.0			0.509	0.631			0.192	0.264
4.0			0.532	0.651			0.225	0.299
6.0				0.641				0.303
8.0				0.622				0.294

Table 7. Normalized stress intensity factor k/k_0 at the deepest penetration point y=0, L=L_0 of an outer semi-elliptic axial surface crack in a cylindrical shell under uniform bending moment M_∞

	L_0 = 0.2h				L_0 = 0.4h			
λ_1	a=h	a=2h	a=4h	a=8h	a=h	a=2h	a=4h	a=8h
0	0.804	0.875	0.926	0.959	0.441	0.579	0.710	0.819
0.5	0.810	0.878	0.927	0.960	0.445	0.590	0.718	0.823
0.75	0.814	0.880	0.929	0.960	0.465	0.598	0.723	0.827
1.0		0.883	0.930	0.961		0.606	0.729	0.831
1.5		0.887	0.932	0.962		0.621	0.740	0.837
2.0			0.934	0.963			0.747	0.842
4.0			0.930	0.961			0.747	0.843
6.0				0.956				0.828
8.0				0.951				0.812
	L_0 = 0.6h				L_0 = 0.8h			
0	0.132	0.238	0.373	0.526	-0.012	0.017	0.065	0.140
0.5	0.143	0.250	0.385	0.536	-0.008	0.022	0.072	0.148
0.75	0.154	0.260	0.394	0.544	-0.003	0.027	0.078	0.155
1.0		0.272	0.405	0.553		0.034	0.085	0.163
1.5		0.295	0.425	0.570		0.047	0.100	0.180
2.0			0.442	0.585			0.115	0.197
4.0			0.464	0.605			0.148	0.232
6.0				0.588				0.231
8.0				0.563				0.217

Table 8. Normalized stress intensity factor k/k_0 at the deepest penetration point $L=L_0$, $y=0$ of an inner semi-elliptic axial surface crack in a cylindrical shell under uniform membrane loading N_∞

	$L_0 = 0.2h$				$L_0 = 0.4h$			
λ_1	a=h	a=2h	a=4h	a=8h	a=h	a=2h	a=4h	a=8h
0	0.817	0.883	0.930	0.961	0.507	0.627	0.741	0.837
0.5	0.813	0.880	0.929	0.960	0.501	0.621	0.737	0.834
0.75	0.810	0.878	0.927	0.960	0.498	0.618	0.734	0.832
1.0		0.876	0.926	0.959		0.615	0.732	0.830
1.5		0.873	0.924	0.958		0.611	0.728	0.827
2.0			0.922	0.957			0.725	0.825
4.0			0.916	0.953			0.718	0.819
6.0				0.950				0.811
8.0				0.946				0.802
	$L_0 = 0.6h$				$L_0 = 0.8h$			
0	0.245	0.336	0.451	0.582	0.073	0.104	0.149	0.216
0.5	0.243	0.333	0.447	0.578	0.074	0.104	0.148	0.215
0.75	0.243	0.331	0.445	0.576	0.075	0.105	0.149	0.215
1.0		0.331	0.443	0.574		0.107	0.150	0.215
1.5		0.333	0.444	0.572		0.112	0.153	0.217
2.0			0.444	0.571			0.158	0.221
4.0			0.451	0.570			0.177	0.237
6.0				0.569				0.242
8.0				0.561				0.241

Table 9. Normalized stress intensity factor k/k_0 at the deepest penetration point $L = L_0$, $y = 0$ of an inner semi-elliptic axial surface crack in a cylindrical shell under uniform bending moment M_∞.

	$L_0 = 0.2h$				$L_0 = 0.4h$			
λ_1	a=h	a=2h	a=4h	a=8h	a=h	a=2h	a=4h	a=8h
0	0.804	0.875	0.926	0.959	0.441	0.579	0.710	0.819
0.5	0.799	0.872	0.924	0.958	0.434	0.573	0.706	0.815
0.75	0.796	0.869	0.923	0.957	0.430	0.568	0.702	0.813
1.0		0.867	0.921	0.956		0.565	0.699	0.811
1.5		0.864	0.919	0.955		0.560	0.694	0.807
2.0			0.917	0.954			0.691	0.805
4.0			0.911	0.950			0.682	0.797
6.0				0.946				0.788
8.0				0.942				0.777
	$L_0 = 0.6h$				$L_0 = 0.8h$			
0	0.132	0.238	0.373	0.526	-0.012	0.017	0.065	0.140
0.5	0.128	0.233	0.368	0.521	-0.012	0.017	0.064	0.139
0.75	0.128	0.231	0.365	0.518	-0.010	0.018	0.064	0.138
1.0		0.230	0.363	0.516		0.019	0.065	0.138
1.5		0.233	0.363	0.513		0.024	0.069	0.141
2.0			0.363	0.513			0.074	0.145
4.0			0.369	0.515			0.091	0.161
6.0				0.507				0.164
8.0				0.495				0.161

Table 10. Distribution of the normalized stress intensity factor k/k_0 along the crack front in a cylindrical shell containing an inner or outer semi-elliptic circumferential surface crack (see insert in Fig. 4), $\lambda_2 = 2$, $a=4h$, $L_0=0.4h$, $\nu=0.3$.

	Outer Crack		Inner Crack	
$\frac{2\phi}{\pi}$	Membrane Loading	Bending	Membrane Loading	Bending
1.0	0.727	0.692	0.685	0.643
0.894	0.719	0.689	0.678	0.641
0.789	0.694	0.680	0.658	0.637
0.684	0.655	0.665	0.625	0.628
0.578	0.604	0.643	0.580	0.615
0.473	0.544	0.618	0.527	0.597
0.367	0.477	0.583	0.465	0.569
0.263	0.406	0.538	0.399	0.529

Table 11. Distribution of the normalized stress intensity factor k/k_0 along the crack front in a cylindrical shell containing an inner or outer axial semi-elliptic surface crack (see insert in Fig. 4), $\nu=0.3$.

	Inner Crack $a=h, R_i=10h, L_0=0.2h$		Inner Crack $a=4h, R_i=10h, L_0=0.8h$		Outer Crack $a=4h, L_0=0.4h, \lambda_1=2$	
$\frac{2\phi}{\pi}$	Tension	Bending	Tension	Bending	Tension	Bending
1.0	0.812	0.799	0.161	0.078	0.773	0.747
0.894	0.807	0.797	0.160	0.082	0.764	0.743
0.789	0.792	0.792	0.157	0.094	0.736	0.731
0.684	0.766	0.782	0.153	0.109	0.693	0.710
0.578	0.730	0.765	0.147	0.124	0.637	0.683
0.473	0.685	0.739	0.138	0.139	0.572	0.652
0.367	0.628	0.700	0.126	0.149	0.500	0.612
0.263	0.559	0.642	0.114	0.154	0.426	0.562

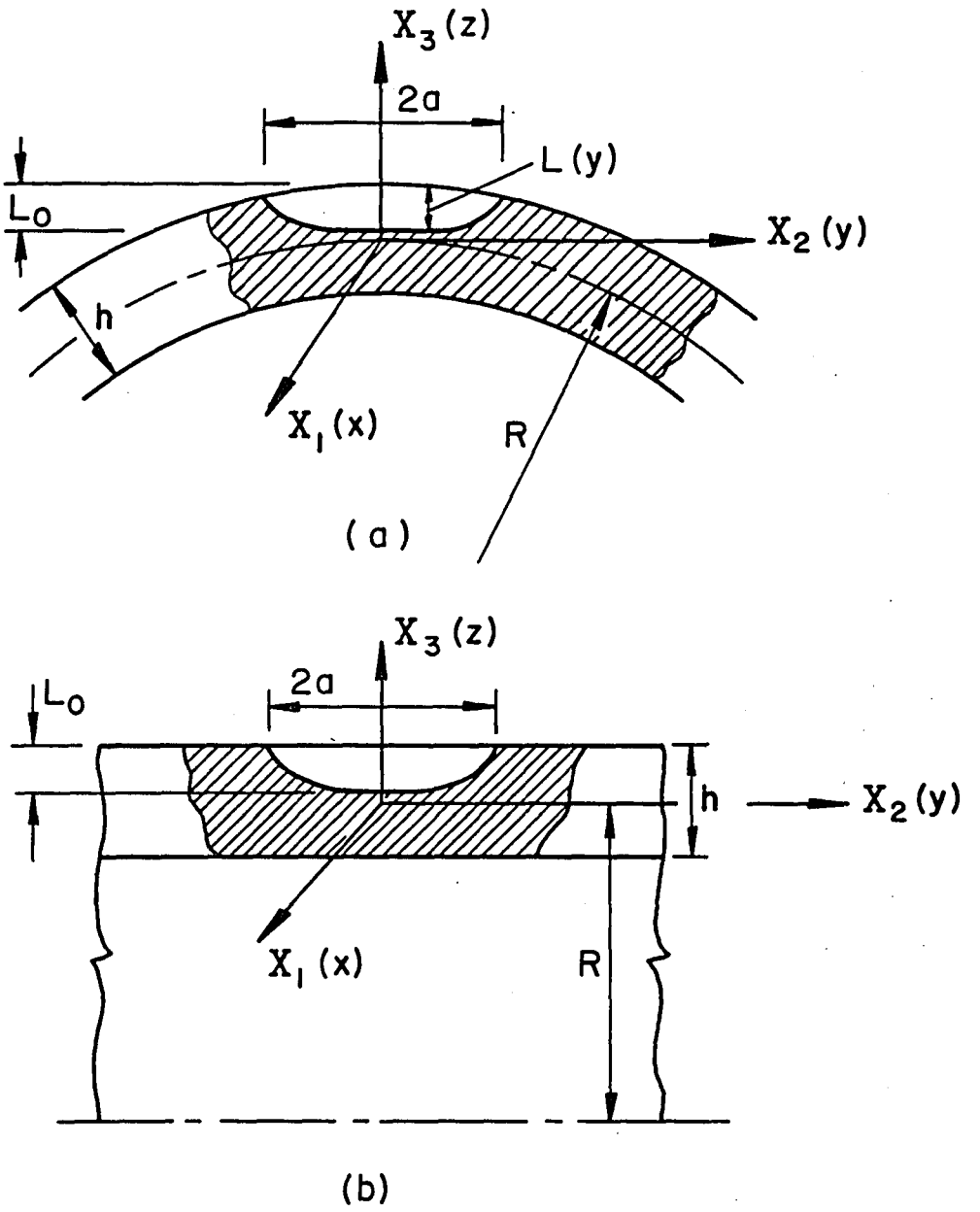

Figure 1. The geometry of a circumferential or an axial part-through surface crack in a cylindrical shell.

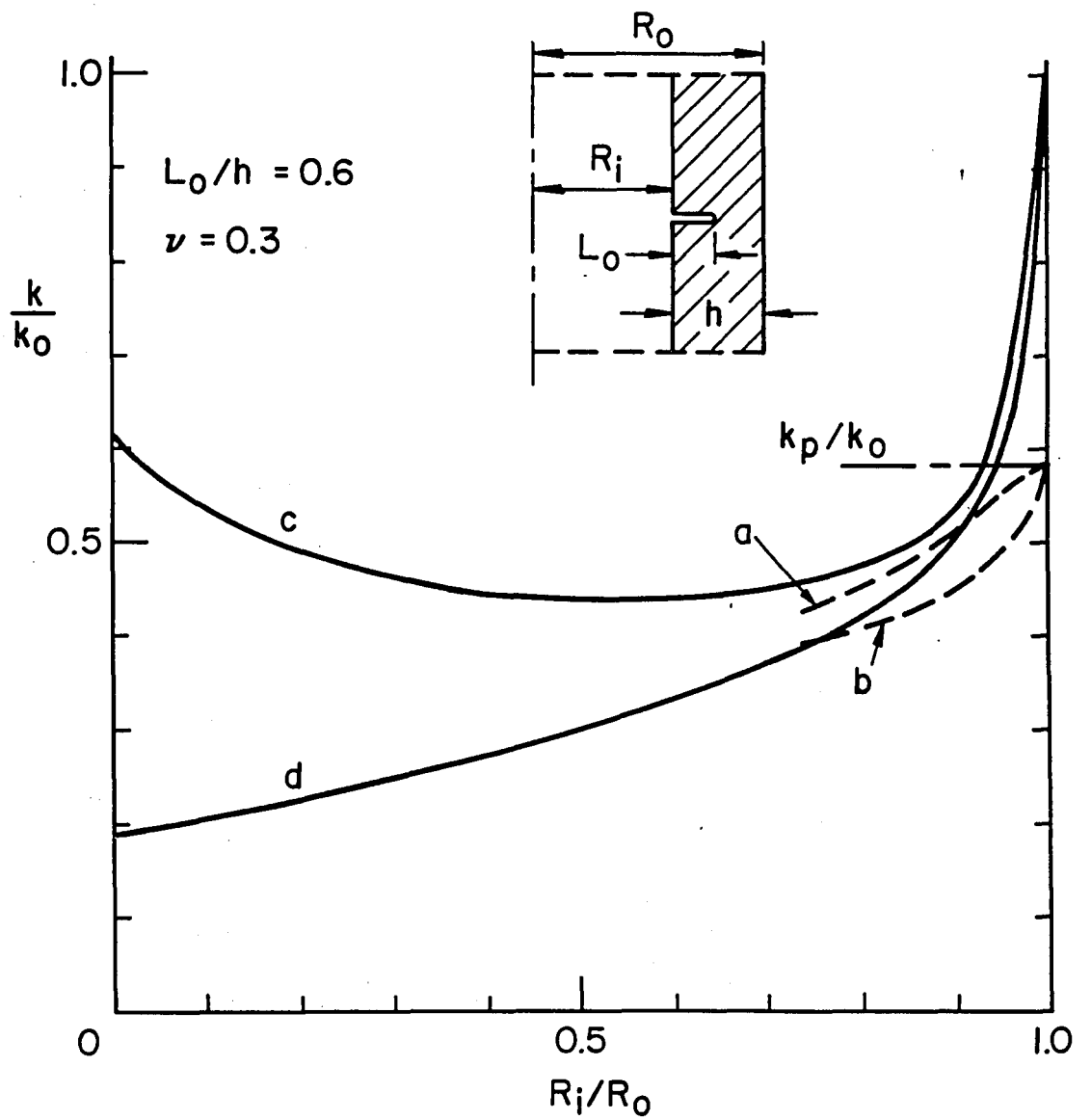

Figure 2. Comparison of the stress intensity factors obtained from the line-spring shell model and the axisymmetric elasticity solution [20]. (a) Stress intensity factor at the deepest penetration point of an external semi-elliptic circumferential crack in the shell, (b) same as (a) for an internal surface crack, (c) elasticity solution for the external axisymmetric crack, (d) the internal axisymmetric crack. (For L_o=0.6h, k_o=4.035 $\sigma_o\sqrt{L_o}$, k_p=0.582 k_o, σ_o: uniform axial stress, a=8h)

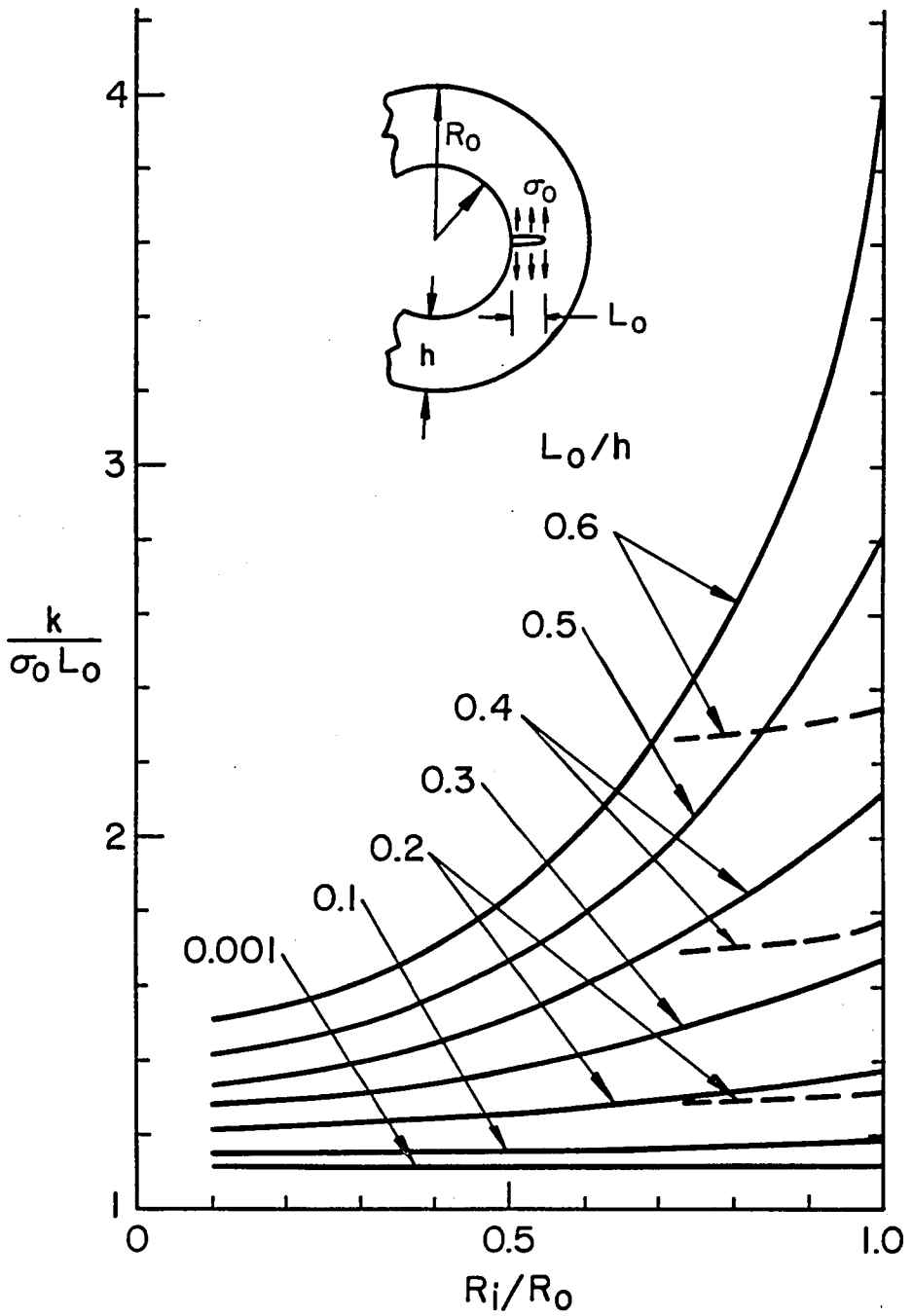

Figure 3. Comparison of the line-spring shell stress intensity factor at the deepest penetration point of an internal axial surface crack (dashed lines) with the corresponding plane strain ring solution (full lines) [18], a=8h

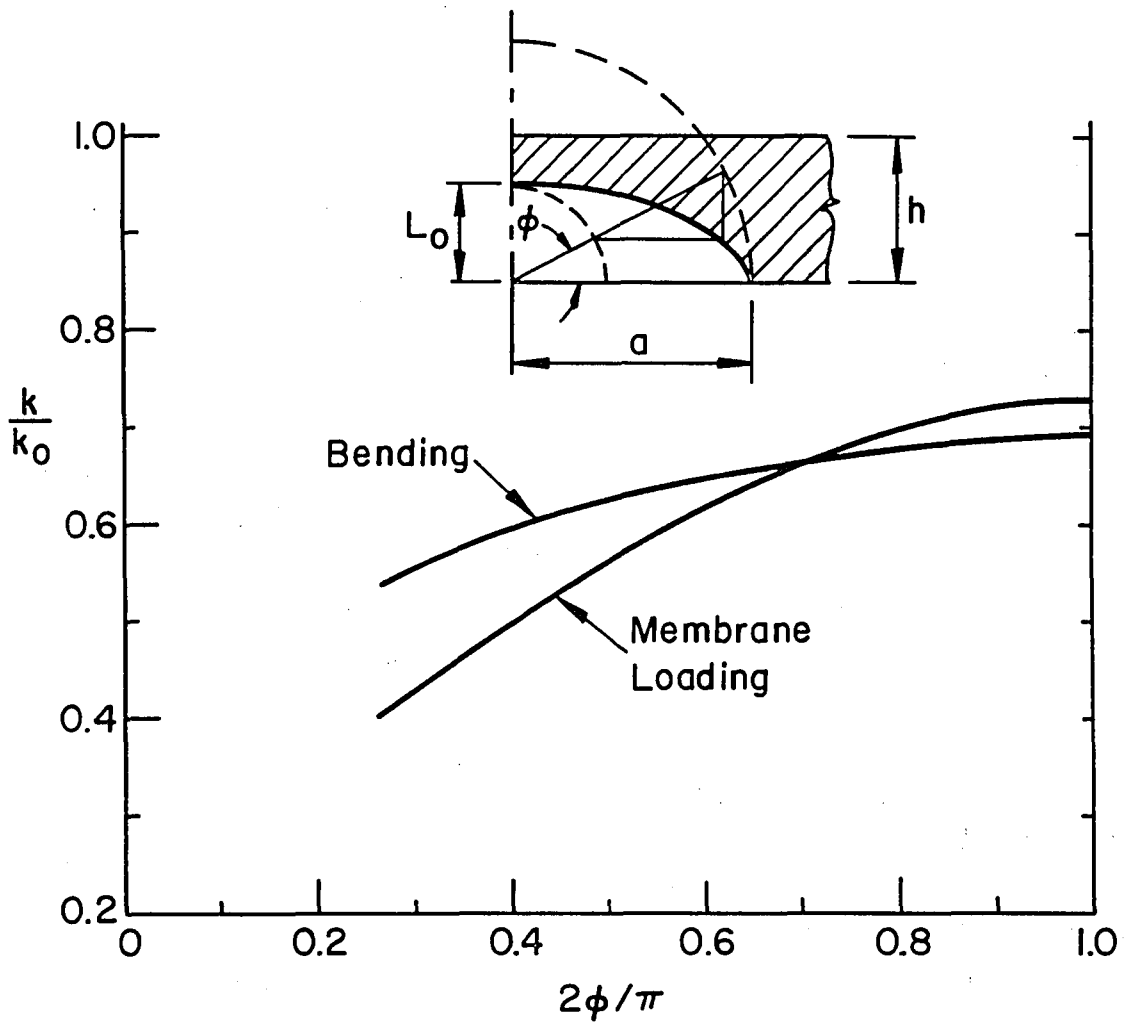

Figure 4. Variation of the stress intensity factor along the front of a semi-elliptic external circumferential surface crack in a cylindrical shell. $\lambda_2 = 2$, $a = 4h$, $L_o = 0.4h$.

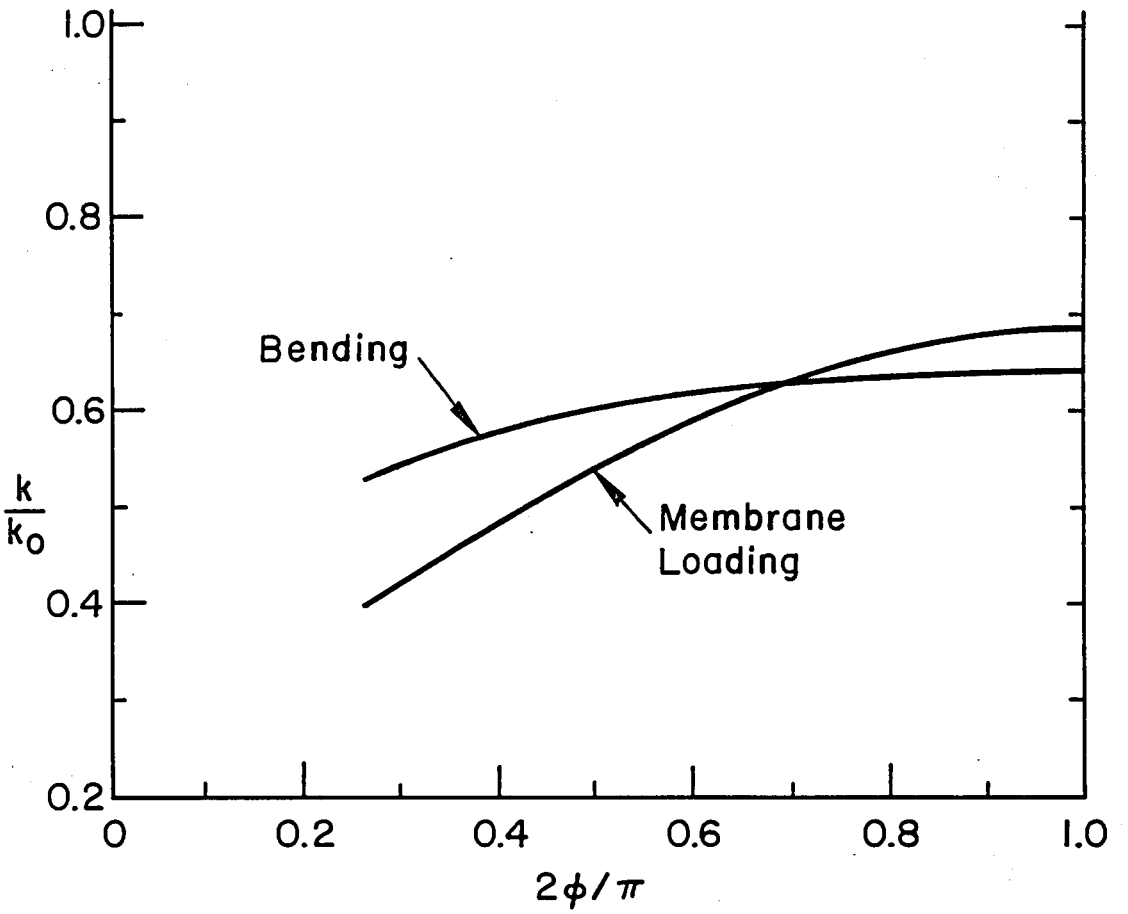

Figure 5. Same as Figure 4, for internal surface crack (λ_2=2, a=4h, L_o=0.4h).

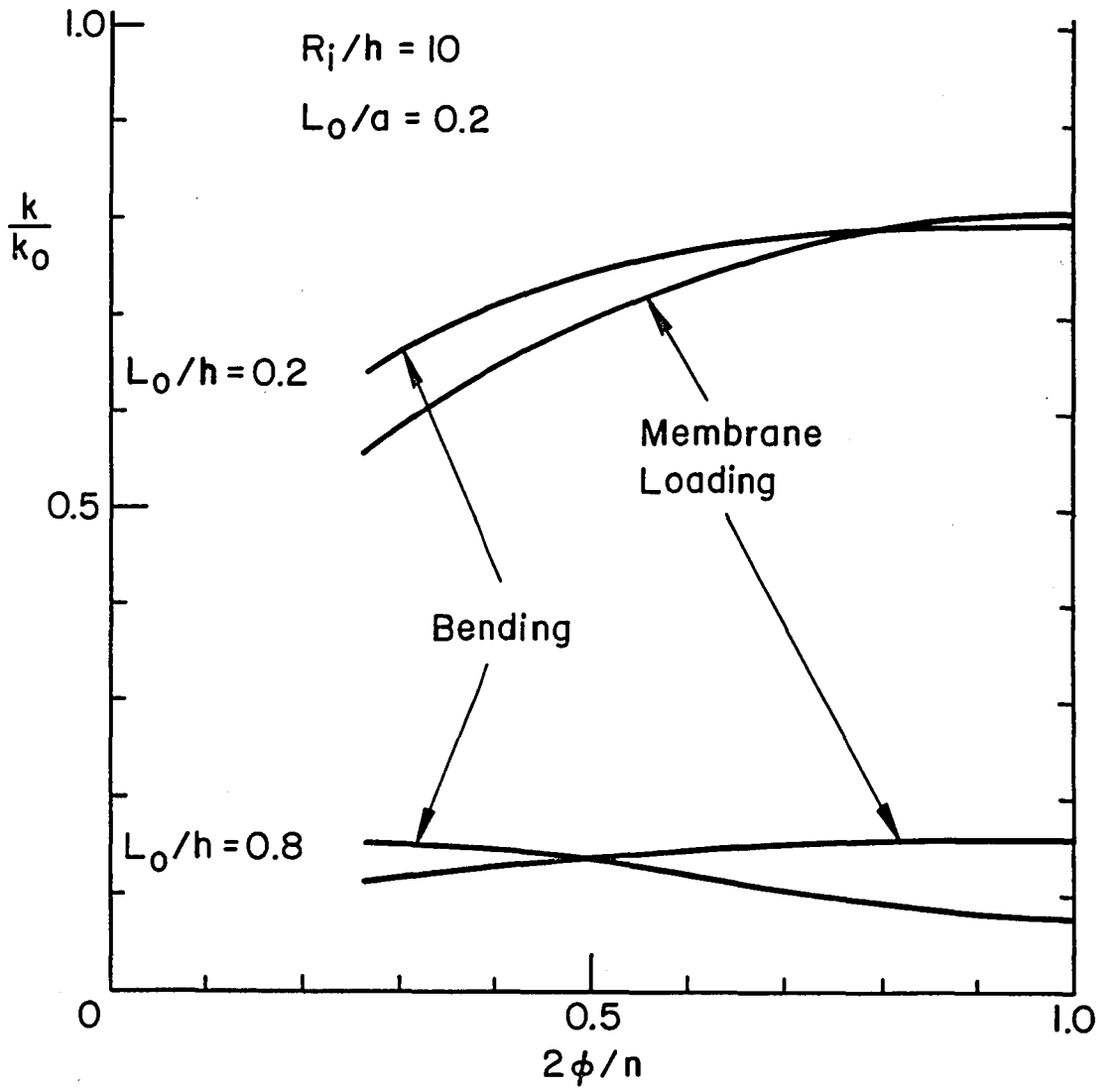

Figure 6. Variation of the stress intensity factor for a semi-elliptic internal axial surface crack in a cylindrical shell.

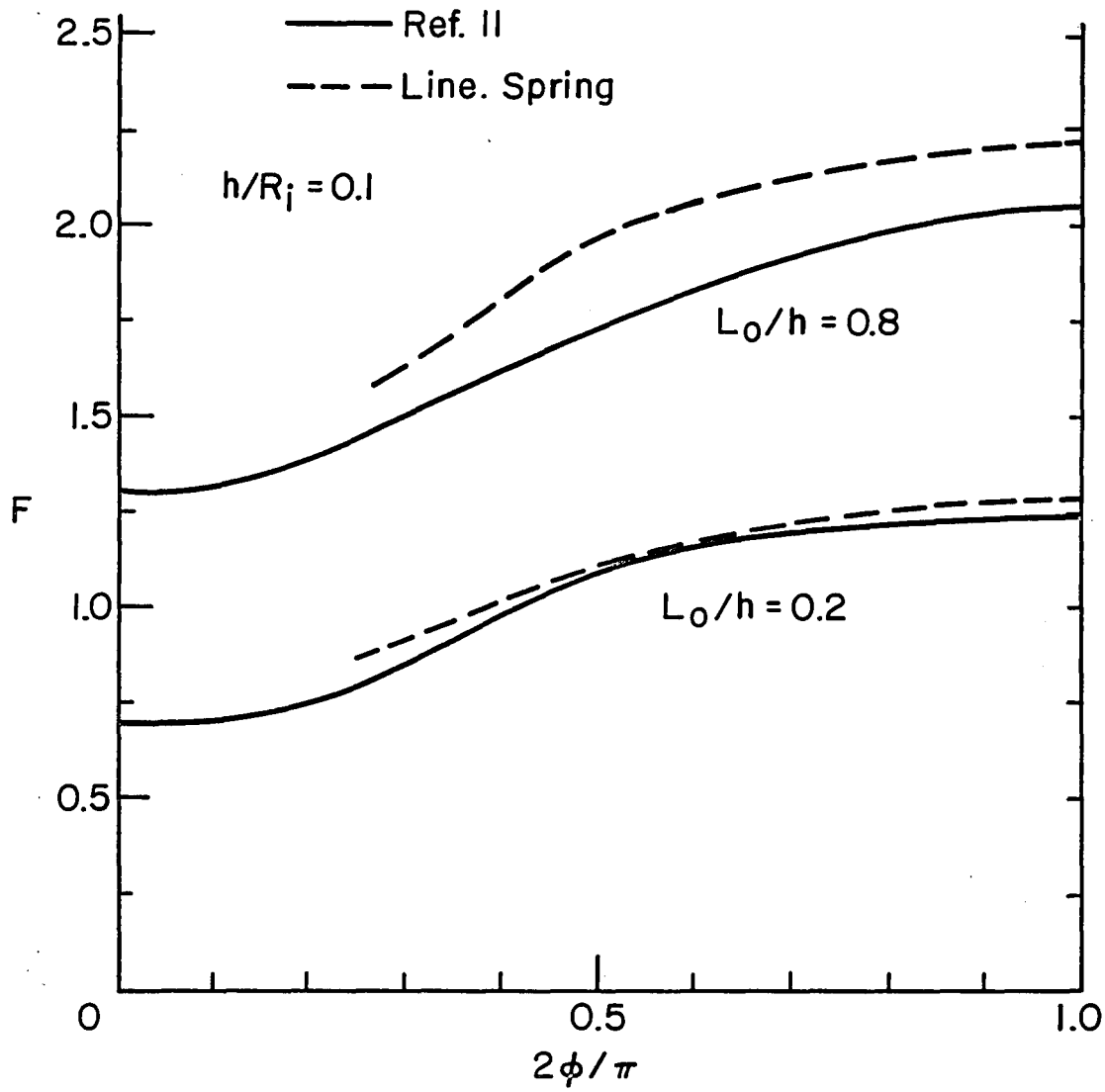

Figure 7. Comparison of the line spring shell results (dashed lines) with the finite element solution (full lines) [14] for a pressurized cylinder containing a semi-elliptic internal axial surface crack.

End of Document